Disentangling the Effects of Intercropping on Vector-Borne Plant-Virus Dynamics

Blake McGrane-Corrigan*, Jon Yearsley

School of Biology and Environmental Sciences, University College Dublin, Belfield, Dublin 4, Ireland

Abstract. Emerging plant diseases threaten crop yields, food security, and the health of ecosystems. In fields with multiple plant species, disease management can become challenging, as different crops can either reduce or increase virus transmission. Motivated by empirical evidence that intercropping can limit virus spread, we develop a mathematical model that integrates the epidemiological dynamics of multiple crops and an insect vector. We derive an explicit expression for the basic reproduction number, showing how infectivity rates and crop composition together determine whether a disease will persist or die out. We also derive a threshold index to assess the potential for transient outbreaks, even when long-term disease persistence is unlikely. We compare monocultures with intercropped systems and find that intercropping does not always reduce disease risk, where, under some conditions, it can actually enhance virus spread. Finally, we explore how crop diversity may shape the evolution of vector host preferences, potentially altering long-term disease risks. These results have practical implications for designing intercropping systems that minimise virus transmission while avoiding unintended amplification effects, providing a theoretical foundation for sustainable and effective plant disease control.

Keywords: disease transmission, host diversity, basic reproduction number, outbreak, transient dynamics, pathogen evolution

1 Introduction

Vector-borne plant viruses are a major concern in agronomy, as they often lead to substantial yield losses and economic damage (Ristaino et al., 2021). Controlling diseases caused by such viruses remains challenging due to the complex interactions among viruses, plant hosts, and insect vectors (Hosack et al., 2008). While insecticides are often used to reduce vector population sizes, their effectiveness can be limited by rapid reinvasion, vector resistance, and negative environmental impacts (Gong et al., 2023). Intercropping, or more broadly polyculturing, is the simultaneous cultivation of multiple crop species within the same field. This agricultural practice has emerged as a possible sustainable strategy that can not only mitigates virus spread but can also strengthen agroecosystem resilience and reduce susceptibility to pest invasions (Grauby et al., 2022; Hooks & Fereres, 2006; Luo et al., 2022; Roudine et al., 2025; Tous-Fandos et al., 2025).

Building on such empirical findings, mathematical modelling offers a complementary quantitative framework that can deepen our understanding of how intercrop traits and management practices influence disease dynamics. This approach can provide insights to optimise intercropping designs and support more targeted field interventions. We present a theoretical

* *Corresponding Author (blake.mcgrane-corrigan@ucd.ie)*

framework that incorporates vector behavior, multi-host infection and transmission dynamics between vectors and crop hosts.

The number of host plants in a field plays a critical role in reducing or amplifying the severity of a disease outbreak. The dilution effect hypothesis proposes that increasing host diversity often reduces disease risk by interrupting transmission pathways (Keesing & Ostfeld, 2021). In contrast, the amplification effect occurs when greater host diversity leads to increased pathogen spread, by raising overall host densities for example. As described by McCann and Gellner (2020), whether dilution or amplification dominates within a system depends on factors such as host competence, community composition, and the mode of transmission. This complexity highlights why it is important to study the effects of intercropping when predicting how biodiversity influences outbreak risk within heterogeneous environments.

Existing theoretical models of intercropping have incorporated spatial structure to assess how crop arrangements influence disease spread (Allen-Perkins & Estrada, 2019; Rosales Herrera et al., 2021; Rother et al., 2025); have focused on specific crop–vector–virus systems to evaluate species-targeted interventions (Cunniffe et al., 2021; Falla & Cunniffe, 2024); or have examined how resistant varieties affect both disease dynamics and crop yield (Vyska et al., 2016). Although these models provide valuable insights into various aspects of vector-mediated plant-virus dynamics, they often consider only a single crop species or do not derive general analytical expressions to guide disease management. The compartmental model we propose tracks virus transmission between multiple host crops and insect vectors, which are in turn either susceptible or infected, enabling us to capture essential transmission dynamics and derive explicit expressions for key epidemic indicators related to both long-term and short-term disease persistence. We present our theoretical framework by using it to answer four applied questions:

Q1 Which intercropping strategies most effectively limit the risk of a plant-virus outbreak?
Q2 When long-term persistence is unlikely, how does intercropping shape short-term outbreak patterns?
Q3 In what ways does intercropping alter outbreak risk comapared to monocultures?
Q4 How might intercropping affect host selective pressures on virus evolution?

To answer Q1 we will first derive the basic reproduction number (a long-term outbreak indicator) and then explore how this quantity behaves under intercrop parameter variation. To answer Q2 we will derive the threshold index of epidemicity (a short-term outbreak indicator) and investigate how this behaves under various intercropping scenarios. We will then answer Q3 by comparing how the basic reproduction number differs between monoculture vs intercropping systems. Lastly, to answer Q4, we will explore evolutionary outcomes by identifying infectivity strategies that maximise the potential for an outbreak. After we answer each of these questions, we will also discuss the ecological consequences of the results and how these may correspond practically to management strategies in each case.

2 The Multi-Host Model

We use an extended Susceptible-Infected approach to model pathogen transmission dynamics in a vector and crop community. Pathogen spread between crops within a field is due to a single vector (typically an insect), where all crops can be a host for this vector. The field system comprises $n \geq 2$ distinct crop species. An individual crop can be either infected or susceptible (i.e. not infected), where $P_{k,I}$ and $P_{k,S}$ are respectively the number of infected and susceptible individuals for crop k). The vector population is likewise divided into susceptible (V_S) and infected (V_I) compartments.

To make interpretation and discussion of our model more direct, which also has a practical focus, we designate species $k = 1$ as a primary crop species of interest, typically a high-value agricultural plant. The remaining species, indexed by $k \in \{2, \ldots, n\}$, represent various intercrops or surrounding non-crop vegetation for example. These intercrops may differ in their epidemiological roles, acting as reservoirs, sinks, or barriers to transmission depending on their susceptibility, infectivity, and attractiveness properties.

The dynamics of infection and recovery in this system are governed by the following system of ordinary differential equations

$$\begin{aligned}
\frac{dP_{k,S}}{dt} &= \mu_k P_{k,I} - \frac{d_k V_I P_{k,S}}{T(P_S, P_I)}, \\
\frac{dP_{k,I}}{dt} &= \frac{d_k V_I P_{k,S}}{T(P_S, P_I)} - \mu_k P_{k,I}, \\
\frac{dV_S}{dt} &= \mu_V V_I - \frac{V_S \sum_{i=1}^{n} c_i P_{i,I}}{T(P_S, P_I)}, \\
\frac{dV_I}{dt} &= \frac{V_S \sum_{i=1}^{n} c_i P_{i,I}}{T(P_S, P_I)} - \mu_V V_I,
\end{aligned} \tag{1}$$

for $k \in \{1, ..., n\}$. The interpretations of parameters in (1) are given in Table 1. Within our model we are ignoring spatial structure and so assume that the arrangement of crop species does not alter the dynamics between susceptible and infected compartments. From the form of 1 we can also see that each crop and vector population has constant total populations sizes, i.e. $P_{k,S}(t) + P_{k,I}(t) = P_k$ and $V_S(t) + V_I(t) = V_T$, for constants $P_k, V_T \geq 0$.

Plant-virus vectors often respond to specific cues, which can be visual, olfactory, or otherwise, and their attraction varies with plant infection status (Falla & Cunniffe, 2024; Pan et al., 2021). This conditional behavior influences whether vectors feed extensively or probe briefly before moving on, with distinct implications for economically harmful viruses, such as persistent and non-persistent viruses in agriculture. For insect pests that transmit such viruses, the likelihood that probing leads to prolonged feeding determines how many crops a vector visits over time, directly affecting transmission potential. With this in mind, we assume that, relative to susceptible crops, vectors can be biased either in favour of ($\nu_k > 1$), or against ($0 \leq \nu_k < 1$), landing on an infected crop of type k (Falla & Cunniffe, 2024). Let $P_S := \{P_{1,S}, ..., P_{n,S}\}$, $P_I := \{P_{1,I}, ..., P_{n,I}\}$. Given that we have n crops, we assume that the probability of infected vectors landing on the kth susceptible crop is

$$\frac{P_{k,S}}{T(P_S, P_I)},$$

where we have that

$$T(P_S, P_I) := \sum_{i=1}^{n} (P_{i,S} + \nu_i P_{i,I})$$

captures the weighted total crop density in the system, which governs how vectors allocate their probing or feeding effort across the community. A similar argument holds for the probability of an infected vector landing on the kth infected crop.

The rate at which susceptible vectors acquire the virus from infected crop k is controlled by the parameter $c_k \geq 0$. The rate at which a susceptible crop k acquires the virus from an infected vector is controlled by the parameter $d_k \geq 0$. We interpret the parameter $\mu_k \geq 0$ as the rate at which infected crops are removed from the system. As total population levels are kept constant, μ_k is also the rate at which infected crops are replenished once removed,

which then enter the susceptible compartment. This removal and replenishment of infected crops is known as roguing Falla and Cunniffe, 2024.

Cunniffe et al. (2021) and Falla and Cunniffe (2024) interpret $\mu_V \geq 0$ as the rate at which a virus vector loses infectivity. This is particularly relevant for so-called non-persistent viruses. Another interpretation, and one that is relevant for persistent viruses, is that this may also be interpreted as the mortality rate of infected vectors, which are in turn replenished as susceptibles. This argument is analogous to the interpretation of μ_k and is justified based on the fact that the total population is constant and on the assumption that there is no vertical transmission of the virus. Throughout this study, unless specifically referred to, we will call μ_V the infective vector loss rate.

Our model builds on previous single-crop (monoculture) plant-virus-vector models (Cunniffe et al., 2021; Falla & Cunniffe, 2024; Madden et al., 2000). These studies highlight key mechanisms, such as vector behavior, virus retention, and host manipulation, that drive disease spread within monoculture systems. Our model extends the base model of Falla and Cunniffe (2024) by looking at the effects of multiple crops on plant-virus dynamics. Falla and Cunniffe (2024) framed their model explicitly in terms of non-persistent virus transmission, where infection can enhance vector activity by increasing the likelihood of vectors landing on infected crops. This mechanism is characteristic of many aphid-borne plant viruses, which can manipulate hosts to facilitate their own spread. However, the general structure of the model (1) is quite flexible and can be applied more broadly to other plant-vector-pathogen systems that exhibit similar ecological phenomena. For example, several fungal pathogens affecting coniferous trees are transmitted by bark beetles, which serve as vectors (Kandasamy et al., 2023). These beetles often preferentially colonise trees that are already infected, guided by olfactory or visual cues emitted by weakened hosts. Such parallels suggest that while the original model is tailored to aphid-virus systems, its underlying mechanisms may be relevant to a wider class of vector-mediated plant diseases.

Parameter	**Interpretation**
c_k	Vector acquisition rate from crop k
d_k	Crop k inoculation rate
P_k	Total number of crops of type k
V_T	Total number of aphids
v_k	Infected crop attractiveness for crop k
μ_k	Roguing rate of crop k
μ_V	Infective vector loss rate
α_k	Transmission effort on crop k
ρ_k	Relative transmission effort deviation for crop k
δ_k	Proportion of crop k
R_0	Basic reproduction number
R_0^C	Baseline potential for disease spread
$\mathcal{E}_0$	Threshold index for epidemicity
r	Amplification envelope

Table 1: Glossary of parameters within (or derived from) the model and their interpretation.

3 Threshold Conditions for Plant-Virus Outbreaks

A central focus in epidemiological modelling is determining when a disease will successfully invade a population. This can be measured mathematically using the basic reproduction number, denoted by R_0, which quantifies the average number of secondary infections caused by a single infected individual in an otherwise susceptible population (Van den Driessche, 2017). While our analysis begins with this threshold quantity, several of our research questions extend beyond it, examining how intercropping modifies infection dynamics relative to monoculture systems, how it affects short-term patterns when potential for long-term disease persistence is low, and how it may shape evolutionary pressures on viral traits. Throughout this paper, we will explore not only conditions for long-term invasion but also the broader ecological and evolutionary implications of intercropping design.

An important property to show for continuous-time models in biological contexts is positivity of solutions, i.e. nonnegative initial conditions result in system trajectories remaining nonnegative for all time. In the Supplementary Material we show that solutions of our system are indeed positive. Since the total populations are constant, we then have that

$$(P_S, P_I, V_S, V_I)^T = (P^*, 0, V_T, 0)^T$$

is the so-called disease-free equilibrium, the steady state of (1) where there are no infected compartments present, where $P^* = (P_1, ..., P_n)^T$.

Given that each total crop population remains constant over time, it suffices to focus on the infected compartments when analysing our model, since we can write $P_{k,S} = P_k - P_{k,I}$ and $V_S = V_T - V_I$. Thus, we reduce our system (1) to

$$\begin{aligned} \frac{dP_{k,I}}{dt} &= \frac{d_k V_I (P_k - P_{k,I})}{\sum_{i=1}^n (P_i + (v_i - 1)P_{l,I})} - \mu_k P_{k,I}, \\ \frac{dV_I}{dt} &= (V_T - V_I)\left(\frac{\sum_{l=n}^n c_i P_{l,I}}{\sum_{i=1}^n (P_i + (v_i - 1)P_{l,I})}\right) - \mu_V V_I. \end{aligned} \tag{2}$$

The dynamics of (2) must stay within realistic bounds, i.e. the infected compartments must not exceed their respective total population sizes. Since each crop and vector population is constant, we have that the set

$$\mathcal{D} := \left\{(P_I, V_I)^T \in \mathbb{R}^{n+1} : 0 \leq P_{k,I} \leq P_k, 0 \leq V_I \leq V_T\right\}$$

is a suitable domain of attraction, where solutions of (2) remain within $\mathcal{D}$ for all $t > 0$.

In order to characterise local stability of the disease-free equilibrium of (2), we computed the basic reproduction number using the next-generation matrix approach (Van den Driessche & Watmough, 2002) as

$$R_0 := r(J_F J_V^{-1}) = \sqrt{\frac{V_T}{P} \sum_{i=1}^n \alpha_i \frac{P_i}{P}}, \tag{3}$$

where $r(A)$ is the spectral radius of a matrix A (maximum modulus over all eigenvalues). The next generation matrix $J_F J_V^{-1}$ is given in the Supplementary Material. In (3) the parameter $P = \sum_{i=1}^n P_i > 0$ is the total number of plants in our system and

$$\alpha_i = \frac{c_i}{\mu_V} \frac{d_i}{\mu_i}$$

represents the virus transmission effort for plant i, assuming that $\mu_V, \mu_i \neq 0$. Specifically, α_i is the product of the rate of aphid infection relative to the vector loss rate and the rate of plant infection relative to plant loss rate. We refer the reader to the Supplementary Material for the derivation of R_0. Note that R_0 is independent of ν_k, the implications of which we will discuss later. It is well known (see Supplementary Material) that if $R_0 < 1$, then the disease-free equilibrium is locally asymptotically stable, meaning all sufficiently small initial infected densities of (1) result in infected trajectories decaying to 0 over time. Conversely, if $R_0 > 1$, the disease-free equilibrium is unstable, and infected trajectories of (1) diverge from 0 in the long run. We conducted several numerical simulations and found that in all observed scenarios, $R_0 < 1$ resulted in disease extinction for all chosen positive initial conditions (see the Supplementary Material for an example), i.e. this may in fact be sufficient for global asymptotic stability of the disease-free equilibrium. From an applied perspective, if a control strategy results in $R_0 = 1$, it does not guarantee disease elimination, additional analysis is needed to determine whether outbreaks will persist or die out. Therefore throughout this paper we will focus on when either $R_0 < 1$ or $R_0 > 1$.

4 Intercropping Strategies that Limit Long-Term Outbreaks

In this section, we will provide some insight into answering Q1. In particular we will explore how different parameters influence disease outbreaks via R_0. We can observe from (3) that in order to ensure an epidemic does not occur for sufficiently small initial infected densities, i.e. $R_0 < 1$, it is necessary that

$$\sum_{i}^{n} \alpha_i \frac{P_i}{P} < \frac{P}{V_T}.$$

This implies that controlling the ratio of total plants to total vectors is critical in limiting disease spread. Specifically, to avoid an epidemic, the average infection gain rate must not exceed the critical threshold given by the plant-to-vector ratio. Controlling either the total vector population size or the infectivity of the host types, via intercropping, can help keep the system below the epidemic threshold. In a monoculture system, controlling the epidemic requires $\alpha_1 < P/V_T$. With intercropping, however, the overall outbreak risk depends on the weighted average infectivity, which is determined by both the total crop population sizes and the viral transmission efforts on each crop. This means that intercropping, with a less susceptible crop can, in general, effectively reduce R_0 below the epidemic threshold even if in a crop-only system there is an outbreak.

4.1 Balancing Virus Transmission Effort

The parameters $\alpha_1, ..., \alpha_n$ represent the virus's transmission effort among crops and are key in determining whether an epidemic can be sustained. For the $n = 2$ case (Fig. 1), the threshold curve $R_0 = 1$ in the (α_1, α_2)-plane separates regions where $R_0 < 1$ and $R_0 > 1$. This threshold curve can be rewritten as

$$\alpha_2 = \frac{P}{P_2}\left(\frac{P}{V_T} - \alpha_1 \frac{P_1}{P}\right). \tag{4}$$

The right-hand side of (4) is a linear, decreasing function of α_1, showing a clear trade-off in transmission effort (see Fig. 1). In particular, we can see from Fig. 1 that higher transmission effort on one plant must be balanced by lower effort on the other to remain below $R_0 = 1$. The intercepts $(\alpha_1^*, 0)$ and $(0, \alpha_2^*)$, where

$$\alpha_k^* = \frac{P}{V_T}\frac{P}{P_k},$$

correspond to the minimal transmission effort, beyond which the system enters an outbreak regime. In higher dimensions, this trade-off generalises to hyperplanes dividing the parameter space into regions of outbreaks and a stable disease-free equilibrium.

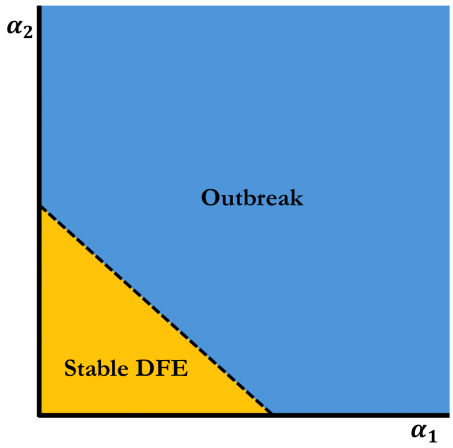

Fig. 1: The (α_1, α_2)-plane showing regions where $R_0 > 1$ (blue) and $R_0 < 1$ (yellow).

4.2 Relative Deviations in Viral Transmission Effort

To better understand the behaviour of R_0 as we vary crop and intercrop parameters, let

$$R_0^C := \sqrt{\alpha_1 \frac{V_T}{P}}$$

be the basic reproduction number of a monoculture system with a total of P plants. Define $\delta_k := P_k/P$ as the proportion of plant type k in the system, and

$$\rho_k := \frac{\alpha_k - \alpha_1}{\alpha_1} = \frac{c_k d_k \mu_1}{c_1 d_1 \mu_k} - 1$$

as the relative deviation in viral transmission effort for crop k, adjusted for loss, compared to the crop plant, respectively (see Table 1). Since $\rho_1 = 0$, the basic reproduction number can be written compactly as

$$R_0 = R_0^C \sqrt{1 + \sum_{i=1}^{n} \rho_i \delta_i}.$$

Note that when all plant types have the same infectivity and roguing parameters as the crop ($\rho_i = 0$ for all $i \geq 2$), we recover $R_0 = R_0^C$. The baseline R_0^C provides a useful benchmark. If it is large, the system may already be conducive to epidemic spread due to factors like high vector density, high transmission efficiency from the crop, or low crop removal rate. Conversely, a small R_0^C indicates low transmission potential from the crop alone. If we let $R_0^1 = R_0^C$ with $P = P_1$, this denotes the basic reproduction number for a single-crop system with P_1 plants. Then we can see that

$$\frac{1}{P_1} > \frac{1}{P} \implies R_0^1 \geq R_0^C,$$

with equality only when no intercrops are present. This highlights that introducing additional plant types may dilute the crop's contribution to disease spread.

4.3 Intercrop Characteristics and Baseline Disease Spread

To better understand and visualise how ρ_i and δ_i alter R_0, we will focus on the $n = 2$ case. Throughout the rest of this paper, when $n = 2$, we will write $\rho := \rho_2$ and $\delta := \delta_2$, for ease of exposition. The influence of R_0^C on R_0 is illustrated in both Fig. 2 and Fig. 3, showing how differences in infection, inoculation and roguing rates between two plant types affect epidemic potential, depending on the value of R_0^C. It is worth highlighting that although δ mainly affects the intercept and steepness of the $R_0 = 1$ curve in Fig. 2, it also corresponds to a practical management intervention. Modifying δ by altering intercrop density can either reduce or increase disease risk, depending on the relative difference transmission effort, ρ. We can see in Fig. 3 that R_0 is a strictly increasing function of ρ, when δ is held fixed. Varying δ changes the ρ-intercept and slope of the curve in Fig. 3. However the specific value of δ does not alter the general behaviour observed in Fig. 3.

From Fig. 2 and Fig. 3 we can deduce the following:

- If $R_0^C = 1$, then this represents a critical baseline transmission potential when $\rho = 0$ (see Fig. 2). In this scenario, if $\rho > 0$, meaning that the intercrop is more conducive to infection than the crop, then $R_0 > 1$ and the disease will always persist. However, if $\rho < 0$, then $R_0 < 1$ and the disease has low potential of establishing. In this case, when the system is balanced in terms of transmission and roguing effort, introducing a less susceptible or more aggressively managed intercrop can prevent an epidemic. Thus, the most effective strategy here would be to introduce an intercrop that is less conducive to infection (via lower α_2 or higher μ_V) to tip the system below $R_0 = 1$.
- If $R_0^C < 1$, then the baseline potential for virus spread is low (when $\rho = 0$). Even if the intercrop is more susceptible or less well managed ($\rho > 0$), the system may still suppress disease spread, so long as ρ is not too large. We can see in Fig. 3 that there also exists $\hat{\rho} > 0$ such that $R_0 > 1$ for all $\rho > \hat{\rho}$. This implies that even modest increases in the susceptibility or mismanagement of the intercrop can tip the system into an epidemic regime. Thus, the most effective strategy here would be to introduce any intercrop with similar or lower susceptibility, but avoid highly susceptible intercrops, which can tip the system into an outbreak regime. If the intercrop is a stronger transmitter of the virus, i.e. $\rho \gg 0$, then if δ is kept low enough, this may prevent an outbreak.
- If $R_0^C > 1$, then we have an outbreak in our crop only system (when $\rho = 0$). Therefore, introducing a similarly or more susceptible intercrop ($\rho > 0$) will only make this worse. However, if the intercrop is less susceptible or more aggressively managed ($\rho < 0$), it may help reduce R_0, but only if this difference is sufficiently large. We can see in Fig. 3 that there also exists a threshold $\tilde{\rho} < 0$ such that $R_0 > 1$ for all $\rho > \tilde{\rho}$. This suggests that strategic deployment of suppressive intercrops can be effective in pushing the system below the epidemic threshold. Thus, the most effective strategy here would be to only introduce a high proportion of intercrops with substantially lower susceptibility or more aggressive management ($\rho \ll 0$).

In Fig. 3, for $x \in \{\hat{\rho}, \tilde{\rho}\}$, and for a given $\delta > 0$ and $R_0^C > 0$, we can write

$$x := \frac{1}{\delta}\left(\frac{1}{(R_0^C)^2} - 1\right).$$

The lines $\rho = \hat{\rho}$ and $\rho = \tilde{\rho}$ respectively describe the threshold beyond which increasing the relative deviation in viral transmission effort results in disease outbreaks when $R_0^C < 1$ and $R_0^C > 1$. The intercropping system tends to be especially sensitive to small changes in parameters near the threshold values $\hat{\rho}$ and $\tilde{\rho}$, emphasising the importance of careful

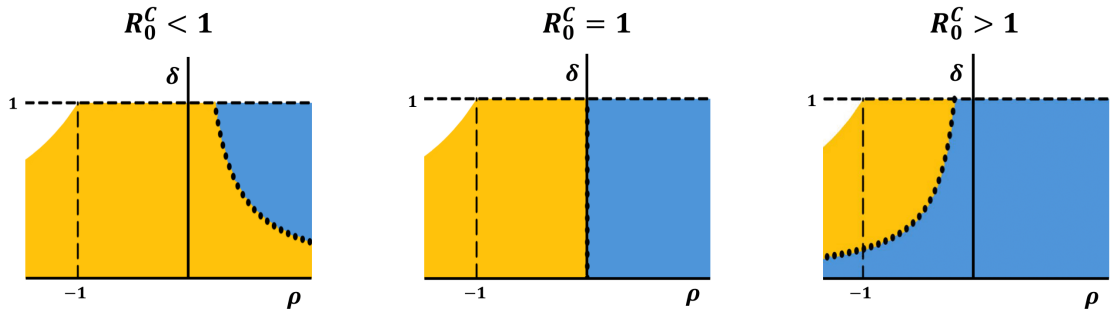

Fig. 2: Behaviour of R_0 in the (ρ, δ)-plane, with $R_0 < 1$ (yellow region), $R_0 = 1$ (black dotted line) and $R_0 > 1$ (blue region) when $R_0^C < 1$ (left), $R_0^C = 1$ (middle), and $R_0^C > 1$ (right). The dashed black lines are $\delta = 1$ (horizontal) and $\rho = -1$ (vertical). The white region is where R_0 undefined when $\rho < 0$.

management to limit disease spread. While actual agricultural environments often include several intercrop species and more complex vector dynamics, this two-plant example offers valuable insights into the effects of intercrop characteristics on outbreak risk.

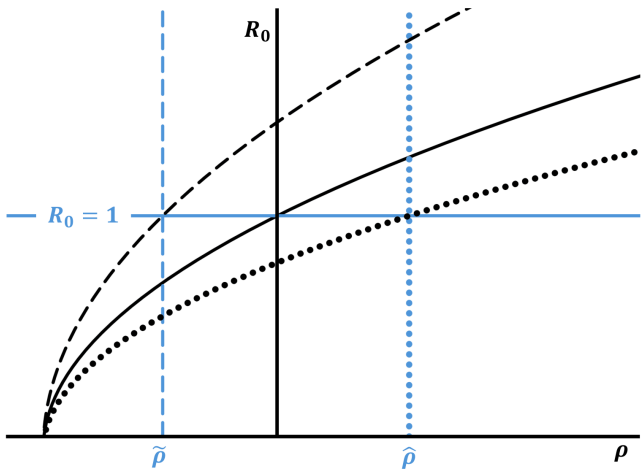

Fig. 3: R_0 as a function of ρ (black lines) for $R_0^C = 1$ (solid), $R_0^C < 1$ (dotted), and $R_0^C > 1$ (dashed). The blue lines are respectively $R_0 = 1$ (solid), $\rho = \hat{\rho}$ (dotted) and $\rho = \tilde{\rho}$ (dashed).

4.4 Implications for Management Strategies

These results theoretically show that intercropping does not inherently suppress virus outbreaks. The epidemiological outcome depends critically on the intercrop's infectivity and management relative to the main crop. In some cases, intercropping may inadvertently increase R_0, if the intercrop acts more as a source of viral transmission than as a suppressive barrier. Grauby et al. (2022) observed that intercropping sometimes has little to no effect on reducing Barley Yellow Dwarf Virus transmission in aphids. This empirical finding highlights the importance of intercrop selection and targeted interventions to achieve effective disease suppression. In some cases crops may promote the development of alate (winged) aphids if the crops attracts and retains an aphid pest that harbours a non-persistent virus. This facil-

itates positive density dependence, inducing aphid dispersal due to intraspecific competition (Carr et al., 2020; Donnelly et al., 2019).

A plausible ecological mechanism observed previously is an induced Allee effect in the vector population (Taylor & Hastings, 2005). At low densities, vectors struggle to find hosts or feed efficiently, and intensive roguing can push their numbers below a critical threshold, with R_0 being reduced below one. However, if vectors can rebound, due to higher overall densities or low removal rates, transmission can rapidly increase. This highlights trade-offs between infectivity rates and suggests that combining intercropping with targeted vector suppression when densities are low can reduce or even prevent outbreaks (Tobin et al., 2011). These results show that effective intercropping can reduce R_0 below the epidemic threshold, limiting disease spread. However, success depends not just on increasing plant diversity, but on the specific susceptibility and management of both crop and intercrop species. Intercrops that transmit infection poorly or are removed quickly suppress R_0, while highly susceptible or poorly managed intercrops can amplify it. Simply adding an intercrop is insufficient, as strategic selection and management are essential in order to reduce R_0 and limit the risk of a plant-virus outbreak.

5 Predicting Transient Outbreaks Despite Disease Extinction

From an applied perspective, population densities are observed over finite time intervals, making short-term dynamics as important as long-term qualitative behaviour determined by R_0 (Li & Zou, 2024). Although $R_0 < 1$ ensures eventual decline of outbreaks for small enough initial densities, it does not rule out transient amplifications, temporary increases in infection following small perturbations or disturbances. For example, an initial surge in infections can still cause significant crop yield losses within a single growing season. This highlights the need for strategies that control transient outbreaks to ensure practical disease suppression. To characterise this behavior, and to provide an answer to Q2, we will analyse our system's reactivity (also known as the epidemicity index), denoted by R_J, which quantifies the initial growth rate of our system following perturbation from the disease-free equilibrium (Arnoldi et al., 2016; Hosack et al., 2008; Trevisin et al., 2022). Reactivity is especially relevant in epidemiology, where short-lived outbreaks can still cause substantial harm despite long-term extinction (O'Regan et al., 2020). Competent intercrops with high transmission rates may increase reactivity and exacerbate transient outbreaks, while poorly competent or non-host intercrops may suppress early infection growth.

5.1 Reactivity and the Epidemicity Index

Positive reactivity corresponds to the largest real eigenvalue of the Hermitian part of the Jacobian matrix at the disease-free equilibrium. The opposite of reactivity, so when $R_J < 0$, is also called initial resilience, where trajectories do not exhibit short-term growth. Although direct computation can be challenging, Hosack et al. (2008) defines $\mathcal{E}_0$ as a threshold index for epidemicity (a) if $\mathcal{E}_0 > 1$, then $R_J > 0$, so the system is reactive; and (b) if $\mathcal{E}_0 < 1$, then $R_J < 0$, so the system is non-reactive. Hosack et al. (2008) showed that the threshold for epidemicity is given by

$$\mathcal{E}_0 := r\left(H(J_F)H(J_V)^{-1}\right),$$

where $H(A)$ is the Hermitian part of a matrix A. The matrix $H(J_F)H(J_V)^{-1}$ is called the maximum next-generation matrix. The quantity $\mathcal{E}_0$ is interpreted as the maximum number of new infections produced by an infective individual at the disease-free equilibrium Hosack et al. (2008). We refer the reader to Hosack et al. (2008) and the Supplementary Material for more details on $\mathcal{E}_0$.

For our model, we can compute that (see Supplementary Material for derivation)

$$\mathcal{E}_0 = \sqrt{\frac{1}{4\mu_V} \sum_i \frac{1}{\mu_i} \left(d_i \frac{P_i}{P} + c_i \frac{V_T}{P} \right)^2}.$$

Similarly to R_0, we can observe that $\mathcal{E}_0$ is also independent of ν_k. Therefore, infected plant bias has no effect on the qualitative short-term outbreak dynamics of (1). We can also see that $\mathcal{E}_0$ increases with total vector abundance V_T and it decreases with infected vector removal rate μ_V. Thus, higher vector abundance increases transient outbreak potential, while a faster infective vector loss rate suppresses it. For $n = 2$, plotting $\mathcal{E}_0$ in the (c_1, c_2)-plane or (d_1, d_2)-plane reveals a pattern similar to how α_i affect R_0 (see Fig. 1). Specifically, large c_k or d_k values correspond to high reactivity (short-term infection growth), while smaller values lead to initial resilience, showing that more efficient virus transmission increases transient outbreak potential.

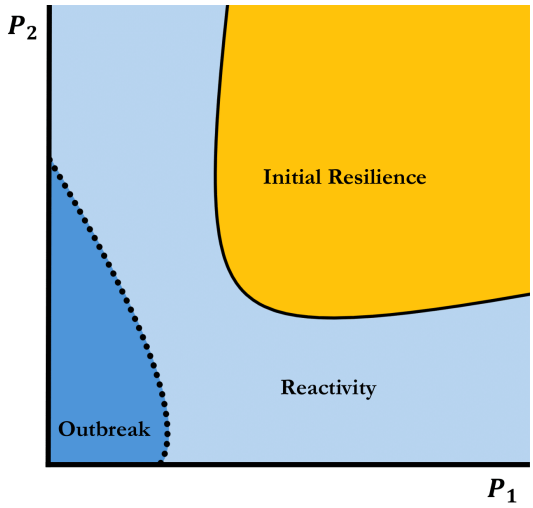

Fig. 4: The (P_1, P_2)-plane showing regions where $\mathcal{E}_0 > 1$ (light blue), $\mathcal{E}_0 < 1$ (yellow), and $R_0 > 1$ (dark blue).

Visualising $\mathcal{E}_0$ in the (P_1, P_2)-plane (Fig. 4) reveals distinct regions of initial resilience, reactivity, and outbreaks. At low total plant densities, outbreaks can occur due to dilution effects, where fewer hosts paradoxically increase transmission efficiency despite lower host availability (Keesing & Ostfeld, 2021). Moderate to high transmission rates shrink the initial resilience region, which is highly sensitive to intercrop traits. In particular, low intercrop transmission rates (e.g., low d_2) substantially reduce transient outbreak potential, especially at high intercrop densities, reflecting patterns seen in R_0. Thus, intercrops with low transmission efficiency enhance initial resilience by preventing early epidemic spikes. Similarly, increasing infected plant or infective vector loss rates (μ_i, μ_V) decreases $\mathcal{E}_0$ and narrows the reactive region, consistent with faster removal limiting transmission opportunities during outbreak onset.

5.2 The Maximum Amplification Envelope

Complementing reactivity is the amplification envelope, defined as

$$r(t) := \| \exp(Jt) \|_2,$$

where $\exp(Jt)$ is the matrix exponential and $\|\cdot\|_2$ is the Euclidean norm. This quantity measures the largest possible amplification of any unit-norm initial perturbation at time t. In practice, $r(t)$ corresponds to the largest singular value of $\exp(Jt)$ and is computed numerically (O'Regan et al., 2020). Over a finite time interval $[0, T]$, we define

$$r_T := \max_{t\in[0,T]} r(t)$$

as the maximum transient growth attained within that interval. To provide time-independent bounds on this transient growth, Townley et al. (2007) recommend using the Kreiss bound, denoted K_J (see the Supplementary Material for more details). This bound offers a time-independent envelope where $\sup_{t\geq 0} r(t)$ lies. There exists algorithms for computing K_J (see, for example, Mitchell (2020)), but this is beyond the scope of the current paper. We included a numerical simulation of the linearised system of (2), for $n = 2$, in the Supplementary Material, showing these various transient bounds.

Assume we have a main crop of interest, where we know the crop transmission rates from both infected vectors, c_1, and plants, d_1. It would be beneficial to know how variation in the intercrop transmission parameters, c_2 and d_2, influences short-term transient outbreaks. To illustrate this, in Fig. 5, we calculated r_T, for $T = 5$, under two contrasting crop transmission scenarios, one with low values of c_1 and d_1, and another with high values. Even in parameter regimes where $R_0 < 1$, we observe extensive regions of the parameter space in which infection dynamics exhibit substantial short-term growth. The magnitude and extent of this growth are highly dependent on the underlying crop transmission rates.

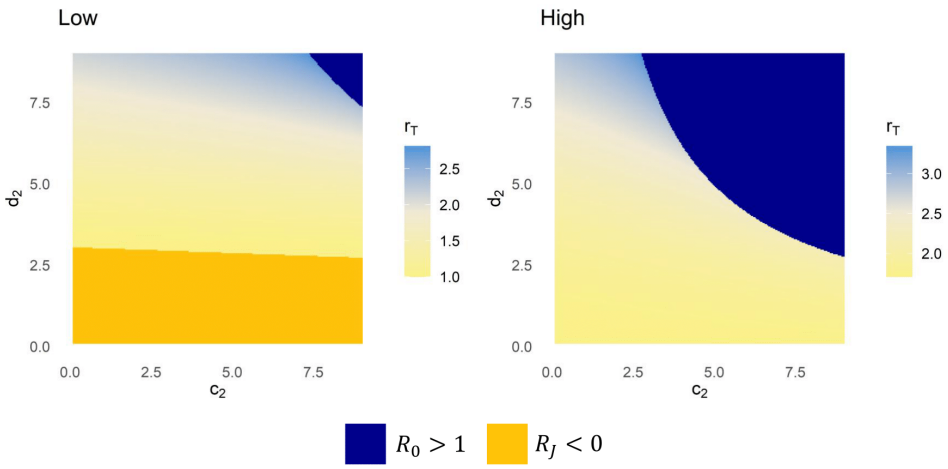

Fig. 5: The (c_2, d_2)-plane showing r_T (yellow-blue gradient) for $T = 5$ time steps, for $c_1 = 0.18$ and $d_1 = 0.64$ (Low) and $c_1 = 6.51$ and $d_1 = 7.62$ (High). Also shown are regions where $R_0 > 1$ (dark blue) and $R_J < 0$ (dark yellow). Parameters: $P_1 = 7397, P_2 = 9443, V_T = 342, \mu_1 = 0.56, \mu_2 = 0.6, \mu_V = 1.26$.

In the low crop transmission scenario, there exists a broad range of c_2 values, with d_2 low to moderate in magnitude, across which the system exhibits initial resilience. However, as plant inoculation rates rise, we see the onset of reactivity, where the system shows initial amplification of infections, even though long-term decay is expected. The magnitude of the maximum amplification envelope increases as both intercrop transmission parameters increase, where transient outbreaks grow, ultimately leading to the emergence of an outbreak regime. In contrast, the high crop transmission scenario markedly reshapes the transient behaviour that is

observed. The region of initial resilience disappears entirely, and reactivity is observed across a much wider range of intercrop parameter values. In this case, even relatively small values of c_2 and d_2 are sufficient to induce transient growth, and the amplification envelope r_T becomes more pronounced as these parameters increase. This ultimately leads to an outbreak regime more rapidly than in the low crop transmission case.

5.3 Implications for Management Strategies

This analysis shows that intercropping can influence not only long-term disease persistence but also short-term outbreak risk. By tuning the total number of intercrop plants and transmission rates, managers can either amplify or dampen transient disease dynamics. High-density intercropping with low transmission efficiency intuitively appears to be most favorable for suppressing both long-term outbreak risk and early transient surges. Conversely, introducing intercrops with high infectivity may backfire, enabling damaging transient outbreaks even when in the long-term one observes extinction. The latter scenario may not be from deliberate planting decisions but could instead arise from unintentional factors, such as the invasion of a novel viral strain or shifts in vector behavior due to environmental conditions.

While R_0 remains an important quantity to characterise, it does not fully capture the risks posed by short-term epidemic spikes in both monoculture and intercropping systems. From an ecological perspective, the results on r_T further underscores the complex interplay between crop and intercrop traits in shaping epidemic potential. Intercrops that are more susceptible or more readily transmit infection to vectors can destabilise the system transiently. The presence or absence of initial resilience reflects how robust the system is to small introductions of infective densities. These findings emphasise the importance of considering not just asymptotic thresholds, but also the transient dynamics that govern early epidemic trajectories in multi-crop communities.

6 Altering Total Crop Sizes in Monoculture vs. Intercropped Fields

In this section, to address Q3, we compare monoculture and intercropping systems by examining how total plant population sizes affect R_0. Specifically, we analyse the relative change in R_0 when introducing intercrops to assess how added host diversity alters epidemic potential. As shown theoretically, intercropping can either enhance or reduce disease spread, depending on crop–intercrop–vector interactions. For intercropping to limit disease, it must increase the average ratio of infection loss to gain rates. We further explore how varying crop and intercrop densities influence disease-free stability and outbreak dynamics, showing that changes in ρ (the relative difference in transmission efforts) can shift intercropping from beneficial to detrimental for disease control as total plant density varies.

We can calculate the relative change in R_0 when we move from a crop-only system ($n = 1$) to a crop-intercrop system ($n \geq 2$) as

$$\Delta R_0 := \frac{R_0 - R_0^1}{R_0^1} = \sqrt{\delta_1 \left(1 + \sum_{i=1}^{n} \rho_i \delta_i\right)} - 1.$$

Note that ΔR_0 is independent of the V_T and μ_V. The effectiveness of intercropping (via ΔR_0) does not depend on vector abundance or loss rate. Thus, management decisions that are based on ΔR_0 are robust to uncertainty in vector population size or infective loss rates. Using this

simplified expression, we will now look at the $n = 2$ case, to investigate how changing P_1 and P_2 affects both R_0 in a monoculture and intercropping system, as well as how ΔR_0 changes, for various fixed ρ. In the Supplementary Material we included particular time series examples of when an unstable disease-free equilibrium (outbreak) in a monoculture system can be stabilised by introducing an intercrop. We also included the opposite behaviour, when a stable disease-free equilibrium in a monoculture system can be destabilised by introducing an intercrop.

6.1 Intercrops as Facilitators of Disease Spread

In Fig. 6, with $\rho > 0$, the intercrop facilitates disease spread more than the crop, possibly by promoting vector movement or increasing contact rates. Different dynamical regimes arise depending on total crop and intercrop densities. When P_1 is low, outbreaks occur in the monoculture and persist at low to intermediate P_2 values, indicating limited disease suppression by the intercrop. As P_2 increases, R_0 initially decreases then rises, but both systems eventually stabilise without outbreaks. At high P_2 values, the system shifts to a stable disease-free equilibrium regime, suggesting that a high total density of intercrops can suppress disease spread despite their facilitation of transmission. Interestingly, an intermediate region shows that adding intercrops may cause outbreaks where the monoculture had a stable disease-free equilibrium, revealing complex crop-intercrop interactions. Finally, at large P_1 and P_2, the disease-free equilibrium stabilises again, likely due to vector limitations in sustaining transmission.

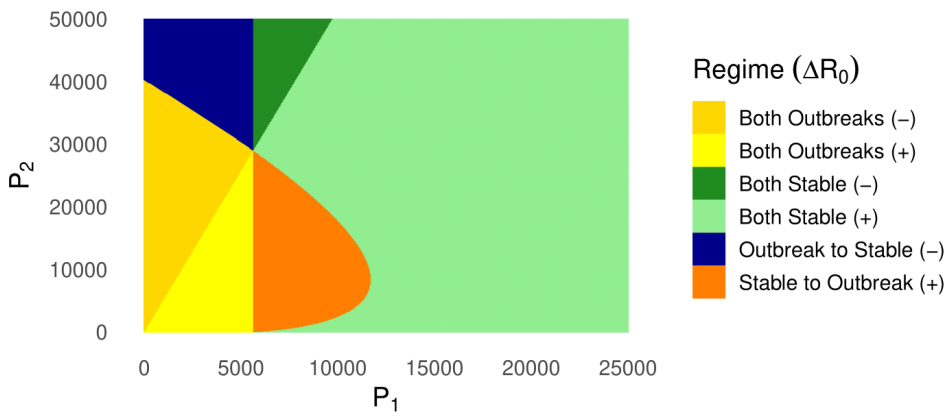

Fig. 6: The (P_1, P_2)-plane for $\rho = 6.14$ showing where the disease-free equilibrium is stable (green) and where outbreaks occur (yellow) for both systems, where we transition from an outbreak to a stable disease-free equilibrium (blue) when moving from monoculture to intercropping, and where we transition from a stable disease-free equilibrium to an outbreak (orange). The sign of ΔR_0 indicates if the transition from monculture to intercropping system is detrimental (dark) or benefical (light). Parameters: $c_1 = 11.86, c_2 = 8.6, d_1 = 4.91, d_2 = 13.31, \mu_1 = 2.18, \mu_2 = 0.6, V_T = 500, \mu_V = 2.37$.

6.2 Intercrops as Barriers to Disease Spread

In Fig. 7, with $\rho < 0$, the intercrop acts as a barrier to disease spread, transmitting infection less effectively than the crop. There is a small region for low enough crop and intercrop densities where outbreaks occur in both monoculture and intercropped fields. Two additional

regions are prominent in this scenario. For low enough crop densities, introducing large densities of intercrops shifts the system from an outbreak under monoculture to a stable disease-free equilibrium, with $\Delta R_0 < 0$, confirming intercropping's beneficial role. When both P_1 and P_2 are large enough, stability is achieved in both systems, likely because the vector population becomes insufficient to maintain transmission across such a large host community.

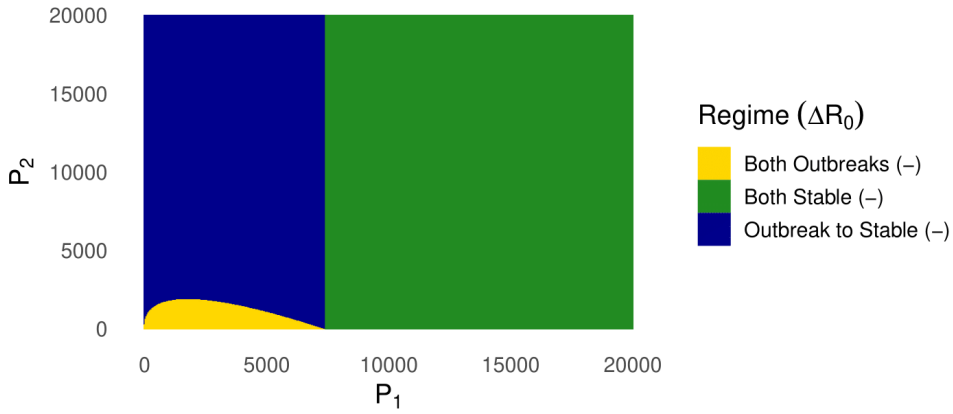

Fig. 7: The (P_1, P_2)-plane for $\rho = -0.96$ showing regimes where the disease-free equilibrium is stable (green) and where outbreaks occur (yellow) for both systems, and where we transition from an outbreak to a stable disease-free equilibrium (blue) when moving from monoculture to intercropping. The negative sign of ΔR_0 in each regime indicates that the transition from monoculture to intercropping system is beneficial. Parameters: $c_1 = 3.65, c_2 = 0.93, d_1 = 9.02, d_2 = 2.37, \mu_1 = 1.25, \mu_2 = 2.31, V_T = 500, \mu_V = 1.78$.

6.3 Implications for Management Strategies

These results align with the ecological concept of dilution effects, as discussed above in the context of transient dynamics, where increasing host diversity reduces disease risk by diluting the impact of highly competent hosts. In addition to these direct effects on transmission, intercropping can influence pathogen dynamics through so-called trait-mediated indirect effects, changes in vector behavior that modify transmission rates without altering host densities (van Veen et al., 2005). Such indirect effects can promote stable coexistence in plant-insect communities by balancing interactions, and in our context, they may inhibit disease spread, which results a healthier susceptible community. Our model captures trait-mediated indirect effects by reflecting how intercrops influence vector behavior alters transmission rates. These behavioral changes can inhibit or facilitate disease spread, with the magnitude of such outbreaks also changing due to infective bias parameters for example (see Supplementary Material). This highlights the importance of considering both direct and indirect effects for effective disease management in intercropping systems.

By quantifying how R_0 changes when moving from monoculture to intercropping systems, we have shown that the epidemiological outcome depends not only on species' transmission competence but also on their relative abundances. When the intercrop is a poor transmitter, increasing its density can lower R_0, stabilising the disease-free equilibrium. However, if the intercrop supports transmission, even modest increases in its population can raise R_0 above the epidemic threshold. Our analysis identifies regions in the (P_1, P_2)-plane where intercrop-

ping either suppresses or promotes spread, emphasising the importance of matching crop choice with appropriate planting densities to avoid unintended amplifications of disease.

7 Intercropping as a Driver of Viral Transmission Adaptation

To understand how a virus may optimise its spread across a heterogeneous environment under our current theoretical framework, and to provide an answer to Q4, we will first examine how it allocates its limited transmission effort among multiple host plant types, each with varying abundance and transmission efficiency. This will make use of the simple expression for R_0.

Viruses that infect multiple host species may evolve adaptive strategies to maximise the potential for an outbreak across these irregular environments. Specifically, they may adjust their transmission effort to optimise disease transmission not only in monocultures, where a single plant type dominates, but also in more complex plant communities. Such adaptations can allow the virus to thrive in diverse ecological settings, enhancing its ability to spread across a range of host types, which is crucial for maintaining virulence and maximising the virus's reproductive success (Gandon, 2004).

Assuming that the virus can flexibly distribute its transmission efforts, $\{\alpha_1, ..., \alpha_n\}$, to favour particular hosts, we seek to determine the allocation that maximises R_0, thereby maximising the potential of an outbreak. We will formalise this as a simple constrained optimisation problem, where the virus invests a fixed total amount of effort across crop types, and aims to maximise its expected transmission success via R_0. Suppose that the virus can modulate its allocation of transmission effort across crop types, such that the total investment remains fixed, i.e. $\sum_{i=1}^{n} \alpha_i = C$ for some constant $C > 0$. From the perspective of the virus, choosing how to distribute transmission effort in order to maximise R_0, increases the potential of such a virus to push R_0 above 1, i.e. induce an outbreak.

By treating each α_i as a variable and all other parameters as constant, the term V_T/P is constant with respect to α_i. Since the square root is strictly increasing, maximising R_0 under the constraint

$$g(\alpha_1, ..., \alpha_n) := \sum_{i=1}^{n} \alpha_i - C = 0$$

is equivalent to maximising the objective function

$$f(\alpha_1, ..., \alpha_n) := \sum_{i=1}^{n} \alpha_i P_i$$

under the same constraint. Applying the method of Lagrange multipliers, we introduce $\lambda \in \mathbb{R}$ and solve $\nabla f = \lambda \nabla g$ (Bertsekas, 2014), which yields $\lambda = P_i$ only if $P_1 = P_2 = \cdots = P_n$. The feasible region,

$$\Omega := \left\{ \alpha \in \mathbb{R}^n : \sum_i \alpha_i = C,\ \alpha_i \geq 0 \right\},$$

is an $(n-1)$-simplex. The linear function f attains its maximum at a vertex of Ω, i.e., where $\alpha_i = C$ for the index i with the largest P_i, and $\alpha_j = 0$ for all $j \neq i$. If all P_i are equal, then f is constant across Ω, and any allocation satisfying the constraint is optimal. Thus, the maximum is not unique and may lie in the interior of Ω. Otherwise, the maximum lies on the boundary. Hence, if we assume that $P_j < P_i$ for all $j \neq i$, then R_0 is maximised when all transmission effort is allocated to the most abundant crop P_i (see Fig. 8 (left) for

an example of this for $n = 3$). Biologically, this suggests that under resource constraints, pathogen evolution may favor specialisation on the dominant host type.

If $P_k = P_l = \hat{P}$, for some $k \neq l$, and all other $P_j < \hat{P}$, for $j \notin \{k, l\}$, then f is maximised by any linear combination of α_k and α_l. This means R_0 is maximised when the virus focuses its transmission effort on the two most abundant hosts. The same conclusion applies if more hosts share the highest abundance (see Fig. 8 (right) for an example for when $n = 3$). The optimal allocation lies on the face of Ω spanned by all equally abundant hosts. Adding less favorable hosts does not alter this consequence, as investing effort in them reduces expected transmission. Thus, the virus evolves to concentrate effort on the most abundant hosts.

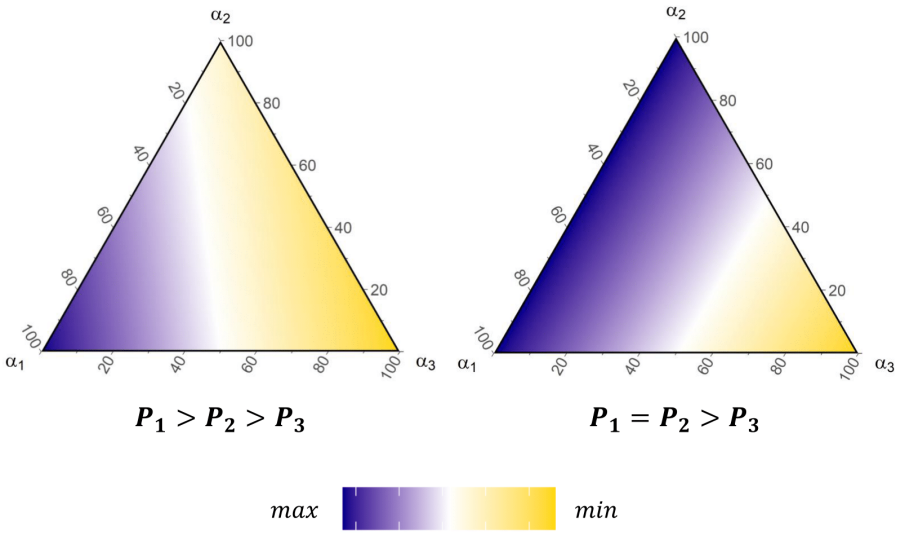

Fig. 8: Three crop example demonstrating the maximal allocation of transmission effort for a range of α_1, α_2 and α_3 in the simplex (triangle) Ω, such that $\sum_i \alpha_i = C > 0$ when (left) $P_1 > P_2 > P_3$ and (right) $P_1 = P_2 > P_3$.

7.1 Implications for Management Strategies

As discussed previously in relation to $\mathcal{E}_0$ and ΔR_0, dilution effects can emerge, whereby increased host diversity reduces the overall risk of disease outbreaks within a community. While this concept has substantial empirical support, there is also evidence indicating the opposite can occur (McCann & Gellner, 2020). Our analysis suggests that when two or more host types are equally abundant, the virus can optimise its transmission by (potentially unequally) distributing it's effort across these hosts, effectively minimising the influence of rare host types. McCann and Gellner (2020) noted that abundant hosts can amplify disease risk for several reasons. Pathogens can face weaker selection pressure to infect rare hosts, and abundant hosts can also tend to allocate more resources to reproduction and fitness than to pathogen defense. Therefore, greater host biodiversity under these conditions may actually promote, rather than inhibit, disease outbreaks. This raises the question of how pathogens allocate their transmission effort when host diversity is high.

Maximising the potential of an outbreak through balancing transmission efforts mirrors the optimal foraging framework described by Charnov's Marginal Value Theorem (Charnov, 1976). Just as foragers optimise their time spent in resource patches to maximise overall intake despite diminishing returns, pathogens face a trade-off where increasing transmission effort yields higher spread but also greater virulence costs that reduce host availability. Our simple analysis, along with our previous results, demonstrate that increasing host diversity can inhibit the evolutionary specialisation of plant viruses on a single crop species. It is well established that monoculture systems are highly vulnerable to pathogen outbreaks due to their genetic uniformity, which facilitate rapid disease spread (Keesing & Ostfeld, 2021). Although we may observe transient outbreak on ecological timescales, intercropping with one or more additional host species introduces heterogeneity into the system, which can act as a buffer against virus proliferation and dominance in the long term. By disrupting transmission pathways and presenting a more complex selective environment, diverse planting strategies may reduce the likelihood of a virus evolving traits that optimise infection and spread within dominant host plants.

It is often assumed that pathogen evolution acts to maximise R_0. However, Lion and Metz (2018) demonstrate that this principle holds only in simplified models where there are little ecological feedbacks. In more realistic host–pathogen systems, complexities such as competitive viral strains or spatial structure, can generate additional feedback loops. Our simple optimisation problem is based on the implicit assumptions that host abundances remain fixed, vector population dynamics are ignored, and the infection processes do not alter the environment in ways that subsequently affect pathogen fitness. Under these conditions, the pathogen's transmission strategy does not change influence the success of future transmission events. Furthermore, transmission parameters like contact rates or vector preferences are assumed to be independent of the current epidemiological state. These assumptions effectively decouple pathogen traits from environmental feedbacks, allowing R_0 to be treated as a direct function of transmission effort. While this is a simplification, it provides a manageable baseline for evaluating intercropping strategies before incorporating ecological nonlinearities found in real-world systems.

8 Discussion

Our theoretical analysis provides key insights into vector-borne plant virus transmission in intercropping systems, showing how pathogen evolution in heterogeneous host environments can alter the potential for disease outbreaks. We derived and interpreted both the asic reproduction number, R_0 and the epidemicity index, $\mathcal{E}_0$, demonstrating that parameters such as ρ_i, capturing relative differences in infectivity, and ΔR_0, the change in reproduction number due to intercropping, offer nuanced understanding of how different intercrop choices alter transmission dynamics. Importantly, our results highlight that intercropping can strongly influence transient epidemic growth. While high-density, low-transmission intercrops can suppress early outbreaks, poorly chosen intercrops may unintentionally amplify short-term epidemic peaks even when long-term persistence is unlikely, i.e. $R_0 < 1$. This complements empirical studies showing intercropping often reduces disease by disrupting vector movement or diluting susceptible hosts (Grauby et al., 2022; Hooks & Fereres, 2006; Luo et al., 2022; Roudine et al., 2025; Tous-Fandos et al., 2025). Our results also imply that in some systems, especially with novel or poorly characterised viruses, intercropping can backfire. For example, if a virus infects multiple hosts or its vector is highly mobile, mixed plantings can increase transmission opportunities and maintain infective vector populations, thus facilitating rather than suppressing epidemics. Overall, these findings underscore that the success of intercropping depends not merely on adding diversity, but on careful selection

of intercrop species based on their ecological and epidemiological roles and interactions with vector behavior. Management strategies that ignore these complexities risk unintended outcomes, whereas intercropping designs informed by mechanistic models such as ours can more effectively enhance sustainability and disease control.

Our study has several limitations that point toward important directions for future research. Mathematically, our analysis focused on local behavior near the disease-free equilibrium, with simulations suggesting threshold dynamics where $R_0 < 1$ leads to extinction for small enough initial infected densities. As mentioned previously, in all observed simulation scenarios we conducted, $R_0 < 1$ resulted in disease extinction for all chosen positive initial conditions. Proving this is the case mathematically, and also providing additional sufficient conditions for global stability for equilibria of (1), remain as open problems. One key simplification of our model is the assumption of a constant total plant and vector population sizes. In natural and agricultural systems, plant populations are dynamic, subject to growth, mortality, and competitive interactions. Introducing explicit population dynamics and plant competition could reveal feedbacks between ecological and epidemiological processes that affect virus persistence. Further realism could also be achieved by parameterising the model for specific crop-virus-vector systems. Spatial scale and the arrangement of crops play a crucial role in shaping disease dynamics, as vector movement and pathogen transmission often depend on the spatial configuration of host plants (Allen-Perkins & Estrada, 2019; McLeish et al., 2017; Rother et al., 2025). Different cropping patterns, such as mixed or row intercropping, create heterogeneous landscapes that may either suppress or enhance virus spread. In practice, virus transmission is also affected by a range of environmental and management factors, such as temperature-dependent vector activity, and the timing and efficacy of insecticide applications, for example (Duffy et al., 2017; Liang et al., 2012). Incorporating such aspects would allow the model to generate more context-specific insights and could inform precision agriculture strategies. Another critical next step is to link this theoretical framework with empirical data. Calibrating the model using field or experimental observations would allow for parameter estimation and validation of predictions (Kendall et al., 1992).

As discussed previously, ν_k does not appear in the expressions for R_0 or $\mathcal{E}_0$. Although this parameter has no influence over the local behaviour of (2) around the disease-free equilibrium, it's influence on system dynamics can be seen when we simulate our model. We simulated our model for $n = 2$, letting ν_1 and ν_2 vary in $(0, 2]$ and found that these parameters can have a beneficial impact on system dynamics in terms of outbreak suppression (see Supplementary Material). In particular, we found that increasing these bias parameters can lower the average infected densities that trajectories tend in the long-run, when in an outbreak regime. These findings highlight the importance of incorporating such conditional vector preferences in longer-term disease management strategies. Falla and Cunniffe (2024) parameterised c_1 in terms of ν_1 for their crop-only system. This was to model non-persistent viruses and how aphids act as vectors for disease transmission. Another potential limitation of our model lies in how general vector preferences are handled. We did not include additional parameters that account for plant-type preference. Some plants may be, in general, more preferable for certain virus species and so incorporating this into our model would be an interesting avenue to take. McElhany et al. (1995) highlighted the relationship between vector behavior and disease spread can also be density-dependent. For example, for Barley Yellow Dwarf Virus, when diseased plants are rare, preference for infected plants promotes transmission, whereas at high disease prevalence, preference for healthy plants has a stronger effect. The use of bias parameters implicitly captures a preference toward susceptible hosts when $\nu_k < 1$. While they may shape the rate of increase/decrease of trajectories (see Supplementary Material), they do not alter the linearised dynamics of our system. Moreover, vector preferences are known

to differ substantially between persistent and non-persistent viruses Cunniffe et al., 2021. Incorporating this into our model may further elucidate how conditional vector preferences affect disease dynamics.

As briefly mentioned, the modelling framework developed in this study is designed with broad applicability in mind, making it well-suited for analysing a diverse array of plant-pathogen-vector systems. For example, it could model the disease dynamics among fruit trees affected by insect-vectored bacterial pathogens, such as *Xylella fastidiosa*, which has had devastating effects on a variety of crop species (Saponari et al., 2019). The same framework can also be applied to cereal crop systems infected by aphid-vectored viruses, where both cultivated grains and surrounding non-crop grasses act as host reservoirs (McElhany et al., 1995). Moreover, in more natural ecosystems, the model has the flexibility to be applied to the spread of forest fungal pathogens facilitated by bark beetles, where different tree species vary in their susceptibility (Kandasamy et al., 2023). This versatility enables the investigation of how vector behavior and host diversity jointly determine epidemic outcomes. By capturing these interactions within a unified framework, the model provides a valuable tool for exploring intercropping and disease dynamics in both managed agricultural systems and heterogeneous natural landscapes, offering insights that are relevant for ecological disease management and conservation planning.

Statements and Declarations

Code Accessibility

All numerical simulations were conducted in R version 4.5.1 (R Core Team, 2025). The code used can be provided upon request.

Funding

Blake McGrane-Corrigan was supported under the Department of Agriculture, Food and Marine (AgriAdapt 2023RP865).

Competing Interests

The authors declare that they have no conflict of interest.

Acknowledgements

We would like to thank Louise McNamara, Stephen Byrne, and Maximilian Schughart for their insightful conversations at the early stages of this project.

References

Allen-Perkins, A., & Estrada, E. (2019). Mathematical modelling for sustainable aphid control in agriculture via intercropping. *Proceedings of the Royal Society A*, *475*(2226), 20190136.

Arnoldi, J.-F., Loreau, M., & Haegeman, B. (2016). Resilience, reactivity and variability: A mathematical comparison of ecological stability measures. *Journal of theoretical biology*, *389*, 47–59.

Bertsekas, D. P. (2014). *Constrained optimization and lagrange multiplier methods*. Academic press.

Carr, J. P., Tungadi, T., Donnelly, R., Bravo-Cazar, A., Rhee, S.-J., Watt, L. G., Mutuku, J. M., Wamonje, F. O., Murphy, A. M., Arinaitwe, W., et al. (2020). Modelling and manipulation of aphid-mediated spread of non-persistently transmitted viruses. *Virus Research*, *277*, 197845.

Charnov, E. L. (1976). Optimal foraging, the marginal value theorem. *Theoretical population biology*, *9*(2), 129–136.

Cunniffe, N. J., Taylor, N. P., Hamelin, F. M., & Jeger, M. J. (2021). Epidemiological and ecological consequences of virus manipulation of host and vector in plant virus transmission. *PLOS Computational Biology*, *17*(12), e1009759.

Donnelly, R., Cunniffe, N. J., Carr, J. P., & Gilligan, C. A. (2019). Pathogenic modification of plants enhances long-distance dispersal of nonpersistently transmitted viruses to new hosts. *Ecology*, *100*(7), e02725.

Duffy, C., Fealy, R., & Fealy, R. M. (2017). An improved simulation model to describe the temperature-dependent population dynamics of the grain aphid, sitobion avenae. *Ecological Modelling*, *354*, 140–171.

Falla, E. K., & Cunniffe, N. J. (2024). Why aphid virus retention needs more attention: Modelling aphid behaviour and virus manipulation in non-persistent plant virus transmission. *PLOS Computational Biology*, *20*(10), e1012479.

Gandon, S. (2004). Evolution of multihost parasites. *Evolution*, *58*(3), 455–469.

Gong, Y., Li, T., Hussain, A., Xia, X., Shang, Q., & Ali, A. (2023). The side effects of insecticides on insects and the adaptation mechanisms of insects to insecticides. *Frontiers in Physiology*, *14*, 1287219.

Grauby, S., Ferrer, A., Tolon, V., Roume, A., Wezel, A., & Jacquot, E. (2022). Can mixed intercropping protect cereals from aphid-borne viruses? an experimental approach. *Insects*, *13*(6), 521.

Hooks, C. R., & Fereres, A. (2006). Protecting crops from non-persistently aphid-transmitted viruses: A review on the use of barrier plants as a management tool. *Virus research*, *120*(1-2), 1–16.

Hosack, G. R., Rossignol, P. A., & Van Den Driessche, P. (2008). The control of vector-borne disease epidemics. *Journal of Theoretical Biology*, *255*(1), 16–25.

Kandasamy, D., Zaman, R., Nakamura, Y., Zhao, T., Hartmann, H., Andersson, M. N., Hammerbacher, A., & Gershenzon, J. (2023). Conifer-killing bark beetles locate fungal symbionts by detecting volatile fungal metabolites of host tree resin monoterpenes. *PLoS Biology*, *21*(2), e3001887.

Keesing, F., & Ostfeld, R. S. (2021). Dilution effects in disease ecology. *Ecology Letters*, *24*(11), 2490–2505.

Kendall, D., Brain, P., & Chinn, N. (1992). A simulation model of the epidemiology of barley yellow dwarf virus in winter sown cereals and its application to forecasting. *Journal of Applied Ecology*, 414–426.

Li, A., & Zou, X. (2024). R 0 may not tell us everything: Transient disease dynamics of some sir models over patchy environments. *Bulletin of Mathematical Biology*, *86*(4), 41.

Liang, J., Tang, S., & Cheke, R. A. (2012). An integrated pest management model with delayed responses to pesticide applications and its threshold dynamics. *Nonlinear Analysis: Real World Applications*, *13*(5), 2352–2374.

Lion, S., & Metz, J. A. (2018). Beyond r0 maximisation: On pathogen evolution and environmental dimensions. *Trends in ecology & evolution*, *33*(6), 458–473.

Luo, K., Zhao, H., Wang, X., & Kang, Z. (2022). Prevalent pest management strategies for grain aphids: Opportunities and challenges. *Frontiers in plant science*, *12*, 790919.

Madden, L., Jeger, M., & Van den Bosch, F. (2000). A theoretical assessment of the effects of vector-virus transmission mechanism on plant virus disease epidemics. *Phytopathology*, *90*(6), 576–594.

McCann, K. S., & Gellner, G. (2020, May). *Theoretical ecology: Concepts and applications*. Oxford University Press.

McElhany, P., Real, L. A., & Power, A. G. (1995). Vector preference and disease dynamics: A study of barley yellow dwarf virus. *Ecology*, *76*(2), 444–457.

McLeish, M., Sacristán, S., Fraile, A., & García-Arenal, F. (2017). Scale dependencies and generalism in host use shape virus prevalence. *Proceedings of the Royal Society B: Biological Sciences*, *284*(1869), 20172066.

Mitchell, T. (2020). Computing the kreiss constant of a matrix. *SIAM Journal on Matrix Analysis and Applications*, *41*(4), 1944–1975.

O'Regan, S. M., O'Dea, E. B., Rohani, P., & Drake, J. M. (2020). Transient indicators of tipping points in infectious diseases. *Journal of the Royal Society Interface*, *17*(170), 20200094.

Pan, L.-L., Miao, H., Wang, Q., Walling, L. L., & Liu, S.-S. (2021). Virus-induced phytohormone dynamics and their effects on plant–insect interactions. *New Phytologist*, *230*(4), 1305–1320.

R Core Team. (2025). *R: A language and environment for statistical computing*. R Foundation for Statistical Computing. Vienna, Austria.

Ristaino, J. B., Anderson, P. K., Bebber, D. P., Brauman, K. A., Cunniffe, N. J., Fedoroff, N. V., Finegold, C., Garrett, K. A., Gilligan, C. A., Jones, C. M., et al. (2021). The persistent threat of emerging plant disease pandemics to global food security. *Proceedings of the National Academy of Sciences*, *118*(23), e2022239118.

Rosales Herrera, D., Ramírez, J., Martínez, M., Cruz-Suárez, H., Fernández Téllez, A., López-Olguín, J. F., & Aragón García, A. (2021). Percolation-intercropping strategies to prevent dissemination of phytopathogens on plantations. *Chaos: An Interdisciplinary Journal of Nonlinear Science*, *31*(6).

Rother, D. C., Cosmo, L. G., Tavella, J., Windsor, F. M., Devoto, M., Evans, D. M., & Guimarães Jr, P. R. (2025). Spatial networks reveal how forest cover decreases the spread of agricultural pests. *Perspectives in Ecology and Conservation*.

Roudine, S., Le Ralec, A., Bouvaine, S., Alford, L., Duval, F., Buchard, C., Llopis, S., Cloteau, R., Georges, R., Jambon, O., et al. (2025). Flower strips in winter reduce barley yellow dwarf virus incidence in cereal crops. *Agriculture, Ecosystems & Environment*, *378*, 109275.

Saponari, M., Giampetruzzi, A., Loconsole, G., Boscia, D., & Saldarelli, P. (2019). Xylella fastidiosa in olive in apulia: Where we stand. *Phytopathology*, *109*(2), 175–186.

Taylor, C. M., & Hastings, A. (2005). Allee effects in biological invasions. *Ecology letters*, *8*(8), 895–908.

Tobin, P. C., Berec, L., & Liebhold, A. M. (2011). Exploiting allee effects for managing biological invasions. *Ecology letters*, *14*(6), 615–624.

Tous-Fandos, A., Chamorro-Lorenzo, L., Caballero-López, B., Blanco-Moreno, J. M., Bragg, D., Casiraghi, A., Pérez-Ferrer, A., & Sans, F. X. (2025). Associating cultivars or species with complementary traits is key for enhancing aphid control through bottom-up effects. *Ecosphere*, *16*(2), e70076.

Townley, S., Carslake, D., Kellie-Smith, O., McCarthy, D., & Hodgson, D. (2007). Predicting transient amplification in perturbed ecological systems. *Journal of Applied Ecology*, 1243–1251.

Trevisin, C., Lemaitre, J. C., Mari, L., Pasetto, D., Gatto, M., & Rinaldo, A. (2022). Epidemicity of cholera spread and the fate of infection control measures. *Journal of the Royal Society Interface*, *19*(188), 20210844.

Van den Driessche, P. (2017). Reproduction numbers of infectious disease models. *Infectious disease modelling*, *2*(3), 288–303.

Van den Driessche, P., & Watmough, J. (2002). Reproduction numbers and sub-threshold endemic equilibria for compartmental models of disease transmission. *Mathematical biosciences*, *180*(1-2), 29–48.

van Veen, F. F., van Holland, P. D., & Godfray, H. C. J. (2005). Stable coexistence in insect communities due to density-and trait-mediated indirect effects. *Ecology*, *86*(12), 3182–3189.

Vyska, M., Cunniffe, N., & Gilligan, C. (2016). Trade-off between disease resistance and crop yield: A landscape-scale mathematical modelling perspective. *Journal of the Royal Society Interface*, *13*(123), 20160451.